Current Control Reference Calculation Issues for the Operation of Renewable Source Grid Interface VSCs Under Unbalanced Voltage Sags

Adrià Junyent-Ferré, *Student Member, IEEE*, Oriol Gomis-Bellmunt, *Member, IEEE*, Tim C. Green, *Senior Member, IEEE*, and Diego E. Soto-Sanchez, *Member, IEEE*

***Abstract*—This paper analyzes the current reference calculation for the control of grid-connected voltage source converters meant to operate under voltage unbalanced sags produced by grid faults. The well-known reference calculation method that allows to control the active power ripple produced by the existence of negative-sequence components in the grid voltage is extensively analyzed. A type of voltage sag that produces unfeasible current reference values is identified and a possible workaround is proposed. Also, the need to compensate the power ripple produced by the filter inductance of the converter is demonstrated and an extension of the calculation method to compensate for this is introduced. The theoretical results are confirmed using simulation tools and experimental tests.**

***Index Terms*—Electric current control, power system faults, three phase electric power, wind energy.**

I. Introduction

VOLTAGE source converters (VSCs) are used in a number of applications ranging from low-voltage microgrid applications [1] to large VSC-HVdc power converters for offshore wind generation [2]. A VSC has been successfully used as a grid connection interface for most renewable energy sources as a doubly fed induction generator (DFIG) and permanent magnet synchronous generator (PMSG) wind turbines and photovoltaic panels. Synchronous reference frame vector control (SRFVC) is the most popular technique for the control of the VSC and has been demonstrated to provide good performance for balanced operation [3], [4].

Increased penetration of renewable energy in the grid has in turn led to increased interest in the development of new methodologies for device control. One important feature is the so-called ride-through capability, which allows the device to remain connected to the grid during different types of grid disturbances and avoid the need to disconnect.

Voltage sags are the most frequent type of grid disturbances. They are reductions of the voltage amplitude and are usually classified between balanced, when the reduction of the voltage is the same for each phase, and unbalanced otherwise. Balanced voltage sags are usually caused by the starting transients of large machines and three-phase short circuits. Unbalanced voltage sags are caused by single-phase or two-phase short circuits and are the most common types of sags [5].

The ride-through capability for balanced voltage sags has been addressed in the past and has been demonstrated by introducing power reduction mechanisms to the SRFVC, as the reduction of the grid voltage causes the converter to reach its maximum allowed current, which in turn causes the voltage of the dc bus to rise due to the excess power input to the bus [6], [7].

On the other hand, ride-through capabilities for unbalanced voltage sags present a number of challenges. The presence of negative-sequence components in the voltage causes a ripple in the power injected to the ac grid . This causes the dc bus voltage to have a ripple, which in some cases may be critical [8]. Also, the existence of negative-sequence voltage causes negative-sequence current to appear, which needs to be controlled to reduce the ripple of the dc bus. The conventional SRFVC is designed to control positive-sequence currents and it exhibits poor performance when controlling the negative sequence [9].

Different choices for alternative designs of the current controllers have been suggested in the past. In [10], a current reference calculation scheme was proposed that enables suppressing the active power oscillations during unbalanced voltage sags using the conventional SRFVC with enhanced current controllers able to track a reference current signals containing both the positive and the negative sequence. In [9], a different current control design with a double SRFVC and independent controllers for positive and negative components was introduced. In [8] and [11], this current control is used for a coordinated control of the back-to-back converter of a DFIG turbine to enable the suppression of the machine torque and the ripple of the dc bus voltage caused by the network unbalances. In [12], a double SRFVC using linear quadratic regulator (LQR) current controllers is proposed for the operation of a PMSG wind

Manuscript received January 19, 2011; revised May 18, 2011 and July 26, 2011; accepted August 24, 2011. Date of current version December 6, 2011. The work of A. Junyent-Ferré and O. Gomis-Bellmunt was supported by the *Ministerio de Ciencia e Innovación* under the project ENE2009-08555. Recommended for publication by Associate Editor S. Williamson.

A. Junyent-Ferré is with the Centre d'Innovació Tecnològica en Convertidors Estàtics i Accionaments (CITCEA-UPC), Departament d'Enginyeria Elèctrica, Universitat Politècnica de Catalunya, ETS d'Enginyeria Industrial de Barcelona, Barcelona 08028, Spain (e-mail: adria.junyent@citcea.upc.edu).

O. Gomis-Bellmunt is with the Centre d'Innovació Tecnològica en Convertidors Estàtics i Accionaments (CITCEA-UPC), Departament d'Enginyeria Elèctrica, Universitat Politècnica de Catalunya, ETS d'Enginyeria Industrial de Barcelona, Barcelona 08028, Spain, and also with the Institute for Energy Research of Catalonia IREC, Barcelona, Spain (e-mail: oriol.gomis@upc.edu).

T. C. Green and D. E. Soto-Sanchez are with the Department of Electrical and Electronic Engineering, Imperial College London, London SW7 2AZ, U.K. (e-mail: t.green@imperial.ac.uk; d.soto-sanchez@imperial.ac.uk).

Digital Object Identifier 10.1109/TPEL.2011.2167761

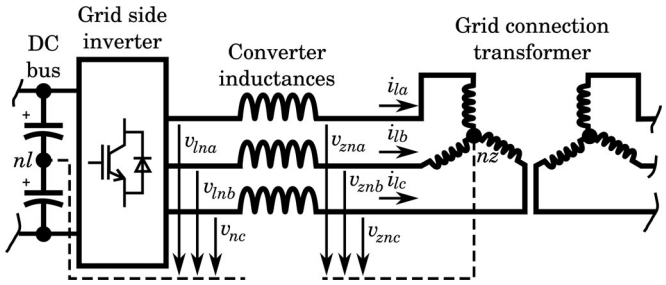

Fig. 1. Grid-connected VSC inverter.

turbine under unbalanced voltage sags. In [13] and [14], the coordinated control of the back-to-back converter of the DFIG using stationary frame current control with proportional-resonant controllers is proposed. The stationary frame control has also been proved to provide good performance under the unbalance operation of VSC, while simplifying the structure of the current controller [15].

The previously mentioned works use current reference calculation methods derived from the one introduced in [10] that uses negative-sequence current injection to compensate the active power oscillations due to the presence of negative sequence in the grid voltage but did not analyze its limitations. This paper focuses on the analysis of this method and provides a critical analysis and some remarks on its limitations and important weak points, which to the best of the knowledge of the authors have not been addressed in the past. Also, modifications of this method that can be used to overcome the weaknesses of this scheme are proposed, tested in simulation, and verified using an experimental test platform.

The paper is organized as follows. The equations needed to model the ac side of the VSC inverter are obtained in Section II. These equations are then, used in Section III to analyze the steady state for balanced operation and to obtain the current reference calculation equations of the conventional vector control. In Section IV, the steady-state equations for the unbalanced operation are obtained and the current reference calculation formulas to control the power output of the converter are derived and discussed. Finally, the conclusions drawn in the previous section are tested on a simulation model in Section V and on an experimental platform in Section VI.

II. Modeling of the Grid-Connected VSC

The basic scheme of a grid-connected VSC is presented in Fig. 1. The purpose of the VSC is to connect a dc bus, which is fed with the power from a renewable generator to the ac grid through a switching device. As the voltage of the dc bus is desired to be constant and the ac grid usually has a low impedance, a filtering inductor is used to connect the switching device to the grid.

The equations that relate the voltage on both sides of the inductor and the current flowing through it can be written as [4]

$$v_{ln}^{abc} + (v_{nl} - v_{nz})\,[1 \quad 1 \quad 1]^T = r_l i_l^{abc} + L_l \frac{d}{dt} i_l^{abc} + v_{zn}^{abc} \tag{1}$$

and

$$i_{la} + i_{lb} + i_{lc} = 0. \tag{2}$$

By combining these equations, the following relation between the voltage of both neutrals is obtained

$$v_{nl} - v_{nz} = \frac{1}{3}\left(v_{zna} + v_{znb} + v_{znc} - v_{lna} - v_{lnb} - v_{lnc}\right). \tag{3}$$

Using this, the voltage equation in (1) can be rewritten in a more compact form as

$$v_l^{abc} = r_l i_l^{abc} + L_l \frac{d}{dt} i_l^{abc} + v_z^{abc} \tag{4}$$

by defining v_l^{abc} and v_z^{abc} as

$$\begin{cases} v_l^{abc} \triangleq v_{ln}^{abc} - (v_{lna} + v_{lnb} + v_{lnc})\,[1 \quad 1 \quad 1]^T \\ v_z^{abc} \triangleq v_{zn}^{abc} - (v_{zna} + v_{znb} + v_{znc})\,[1 \quad 1 \quad 1]^T. \end{cases} \tag{5}$$

Note that (2) assumes that

$$\begin{cases} v_{la} + v_{lb} + v_{lc} = 0 \\ v_{za} + v_{zb} + v_{zc} = 0. \end{cases} \tag{6}$$

To obtain the steady-state equations, it is useful to introduce the Park's variable change matrix. This matrix, for a given Park's reference angle θ, is defined as [16]

$$T(\theta) = \frac{2}{3}\begin{bmatrix} \cos(\theta) & \cos\left(\theta - \frac{2\pi}{3}\right) & \cos\left(\theta + \frac{2\pi}{3}\right) \\ \sin(\theta) & \sin\left(\theta - \frac{2\pi}{3}\right) & \sin\left(\theta + \frac{2\pi}{3}\right) \\ \frac{1}{2} & \frac{1}{2} & \frac{1}{2} \end{bmatrix}. \tag{7}$$

The $qd0$ reference frame representation $x^{abc}(t)$ of a generic $x^{abc}(t)$ signal in the Park reference frame with θ angle is defined as

$$x^{qd0} \triangleq T(\theta) x^{abc}. \tag{8}$$

Introducing the variable change to the system equation (4), it can be rewritten as a function of the new variables

$$v_l^{qd} = \begin{bmatrix} r_l & L_l\dot{\theta} \\ -L_l\dot{\theta} & r_l \end{bmatrix} i_l^{qd} + L_l \frac{d}{dt} i_l^{qd} + v_z^{qd}. \tag{9}$$

Note that the use of the Park reference frame allows suppression of the 0 component equation, which is redundant as $i_{l0} \equiv 0$ according to (2).

III. Analysis of the Current Reference Calculation for Balanced Operation

According to [17], a generic $x^{abc}(t)$ three-phase positive-sequence signal is a function of time that can be described as

$$x^{abc}(t) = \sqrt{2}X \begin{bmatrix} \cos(\omega_e t + \varphi_x) \\ \cos\left(\omega_e t + \varphi_x - \frac{2\pi}{3}\right) \\ \cos\left(\omega_e t + \varphi_x + \frac{2\pi}{3}\right) \end{bmatrix}. \tag{10}$$

By choosing $d\theta/dt = \omega_e$ for the Park reference angle, the transformed signal becomes a vector of constants

$$x^{qd0}(t) = T(\omega_e t + \varphi)x^{abc} = \sqrt{2}X \begin{bmatrix} \cos(\varphi_x - \varphi) \\ -\sin(\varphi_x - \varphi) \\ 0 \end{bmatrix}. \quad (11)$$

We define

$$\begin{bmatrix} x_q^{ss} \\ x_d^{ss} \end{bmatrix} \triangleq \begin{bmatrix} \sqrt{2}X\cos(\varphi_x - \varphi) \\ -\sqrt{2}X\sin(\varphi_x - \varphi) \end{bmatrix}. \quad (12)$$

Considering a balanced case, where both the inverter voltage v_l^{abc} and the grid voltage v_z^{abc} are positive-sequence signals, choosing θ to match the angle of v_{za}, and assuming the derivatives of the current to become zero in the steady state, the following relations can be obtained from (9)

$$\begin{cases} v_{lq}^{ss} - v_{zq}^{ss} = r_l i_{lq}^{ss} + L_l \omega_e i_{ld}^{ss} \\ v_{ld}^{ss} = r_l i_{ld}^{ss} - L_l \omega_e i_{lq}^{ss}. \end{cases} \quad (13)$$

These equations can be used to solve for the current needed to have a certain steady-state power. According to [18], active and reactive powers can be calculated using the voltage and current in the qd form as

$$\begin{cases} P = \dfrac{3}{2}(v_q i_q + v_d i_d) = \dfrac{3}{2}\{v^{qd}\}^T \begin{bmatrix} 1 & 0 \\ 0 & 1 \end{bmatrix} i^{qd} \\ Q = \dfrac{3}{2}(v_q i_d - v_d i_q) = \dfrac{3}{2}\{v^{qd}\}^T \begin{bmatrix} 0 & 1 \\ -1 & 0 \end{bmatrix} i^{qd}. \end{cases} \quad (14)$$

Substitute for the grid connection point

$$\begin{cases} P_z = \dfrac{3}{2} v_{zq} i_{lq} \\ Q_z = \dfrac{3}{2} v_{zq} i_{ld}. \end{cases} \quad (15)$$

Assuming v_{zd} to be zero, which can be ensured by an adequate tracking of the grid voltage measure using a phase locked loop (PLL), (15) implies that active and reactive powers are proportional to i_{lq} and i_{ld}, respectively. This is commonly used to calculate a current reference value for the current control from a power reference signal usually generated by the dc bus voltage regulator and a reactive power command:

$$\begin{cases} i_{lq}^* = \dfrac{2}{3}\dfrac{P_z^*}{v_{zq}} \\ i_{ld}^* = \dfrac{2}{3}\dfrac{Q_z^*}{v_{zq}}. \end{cases} \quad (16)$$

One drawback of this reference calculation method is that it ignores the power loss due to the resistance of the converter filter and its dynamic behavior. Thus, even having a perfect current control, the active power output of the converter P_l will not be equal to the power on the grid connection point P_z and the dc bus voltage regulator will need to be able to compensate for that difference. Usually, this is not a important issue as the filter resistance is small and the regulators used to control the dc bus are designed for disturbance rejection. On the other hand, one possible workaround to match the dc bus voltage regulator power command to the actual power output by the inverter in the steady state is to subtract the losses due to the filter to the active power reference value

$$P_z^* = P_l^* - r_l((i_{lq}^*)^2 + (i_{ld}^*)^2). \quad (17)$$

Note that i_{lq}^* and i_{ld}^* depend on the choice of P_z^*. As the losses due to filter resistance will be very small in comparison with P_l^*, the actual solution may be close to the initial guess P_l^*; thus, one possible approach is to iteratively solve for the current as

$$\begin{cases} (i_{lq}^*)_{n+1} = \dfrac{2}{3}\dfrac{(P_z^*)_n}{v_{zq}} \\ (i_{ld}^*)_{n+1} = \dfrac{2}{3}\dfrac{(Q_z^*)_n}{v_{zq}} \end{cases} \quad (18)$$

with

$$(P_z^*)_n = P_l^* - r_l((i_{lq}^*)_n^2 + (i_{ld}^*)_n^2). \quad (19)$$

IV. Analysis of the Current Reference Calculation for Unbalanced Operation

According to [17], a three-phase signal with positive- and negative-sequence components can be described as

$$x^{abc}(t) = x_+^{abc}(t) + x_-^{abc}(t) \quad (20)$$

where

$$x_+^{abc}(t) = \sqrt{2}X^+ \begin{bmatrix} \cos(\omega_e t + \varphi_x^+) \\ \cos\left(\omega_e t + \varphi_x^+ - \dfrac{2\pi}{3}\right) \\ \cos\left(\omega_e t + \varphi_x^+ + \dfrac{2\pi}{3}\right) \end{bmatrix} \quad (21)$$

$$x_-^{abc}(t) = \sqrt{2}X^- \begin{bmatrix} \cos(\omega_e t + \varphi_x^-) \\ \cos\left(\omega_e t + \varphi_x^- + \dfrac{2\pi}{3}\right) \\ \cos\left(\omega_e t + \varphi_x^- - \dfrac{2\pi}{3}\right) \end{bmatrix}. \quad (22)$$

Unlike in the balanced case, here it is not possible to transform the time-varying signal $x^{abc}(t)$ into a constant signal by using the Park variable change matrix. On the other hand, it is possible to decompose the system into two decoupled systems corresponding to the positive and the negative sequences, which can be analyzed using the same procedure as in the balanced case due to the linear properties of the dynamics of the system and the symmetrical nature of its impedances [17].

The positive-sequence magnitudes can be transformed into constant signals by choosing a Park reference angle matching the angle of the a phase of the original signal

$$x_+^{qd}(t) = T(\omega_e t + \varphi^+)x_+^{abc}(t) = \sqrt{2}X^+ \begin{bmatrix} \cos(\varphi_x^+ - \varphi^+) \\ -\sin(\varphi_x^+ - \varphi^+) \end{bmatrix} \quad (23)$$

while the negative-sequence magnitudes can be transformed into constants by choosing θ to be equal to the angle of the a phase

multiplied by -1

$$x_-^{qd}(t) = T(-\omega_e t - \varphi^-)x_-^{abc}(t) = \sqrt{2}X^- \begin{bmatrix} \cos(\varphi_x^- - \varphi^-) \\ \sin(\varphi_x^- - \varphi^-) \end{bmatrix}. \tag{24}$$

As in the balanced case, we define the steady-state components in the synchronous reference frame as

$$\begin{bmatrix} x_q^+ \\ x_d^+ \end{bmatrix} \triangleq \begin{bmatrix} \sqrt{2}X^+ \cos(\varphi_x^+ - \varphi^+) \\ -\sqrt{2}X^+ \sin(\varphi_x^+ - \varphi^+) \end{bmatrix} \tag{25}$$

and

$$\begin{bmatrix} x_q^- \\ x_d^- \end{bmatrix} \triangleq \begin{bmatrix} \sqrt{2}X^- \cos(\varphi_x^- - \varphi^-) \\ \sqrt{2}X^- \sin(\varphi_x^- - \varphi^-) \end{bmatrix}. \tag{26}$$

Also, as in the balanced case, the steady-state equations can be obtained from (9) by assuming the derivatives of the current to be zero:

$$\begin{cases} v_{lq}^+ - v_{zq}^+ = r_l i_{lq}^+ + L_l \omega_e i_{ld}^+ \\ v_{ld}^+ = r_l i_{ld}^+ - L_l \omega_e i_{lq}^+ \end{cases} \tag{27}$$

and

$$\begin{cases} v_{lq}^- - v_{zq}^- = r_l i_{lq}^- - L_l \omega_e i_{ld}^- \\ v_{ld}^- = r_l i_{ld}^- + L_l \omega_e i_{lq}^-. \end{cases} \tag{28}$$

As for the power equations (14), they include multiplications between voltage and current; thus they are not linear and it is no longer possible to separate positive and negative sequences, as there will be crossed products of terms from both. To calculate the power, the steady-state positive- and negative-sequence magnitudes are transformed to a common reference frame with $\theta = 0$ as

$$P = \frac{3}{2}\{R(-\omega_e t - \varphi^+)v_+^{qd} + R(\omega_e t + \varphi^-)v_-^{qd}\}^T \cdot \begin{bmatrix} 1 & 0 \\ 0 & 1 \end{bmatrix} (R(-\omega_e t - \varphi^+)i_+^{qd} + R(\omega_e t + \varphi^-)i_-^{qd}) \tag{29}$$

and

$$Q = \frac{3}{2}\{R(-\omega_e t - \varphi^+)v_+^{qd} + R(\omega_e t + \varphi^-)v_-^{qd}\}^T \cdot \begin{bmatrix} 0 & 1 \\ -1 & 0 \end{bmatrix} (R(-\omega_e t - \varphi^+)i_+^{qd} + R(\omega_e t + \varphi^-)i_-^{qd}) \tag{30}$$

where $R(\theta)$ is a rotation matrix defined as

$$R(\theta) = \begin{bmatrix} \cos(\theta) & -\sin(\theta) \\ \sin(\theta) & \cos(\theta) \end{bmatrix}. \tag{31}$$

Note that it can easily be proven that the following relation exists between $T(\theta)$ and $R(\theta)$:

$$T(\theta) \equiv \begin{bmatrix} R(\theta) & 0 \\ 0 & 1 \end{bmatrix} T(0). \tag{32}$$

The resulting equation of the active power can be written as

$$P = P_0 + P_{\cos}\cos(2\omega_e t + \varphi^+ + \varphi^-) + P_{\sin}\sin(2\omega_e t + \varphi^+ + \varphi^-) \tag{33}$$

where

$$\begin{cases} P_0 = \frac{3}{2}\left(v_q^+ i_q^+ + v_d^+ i_d^+ + v_q^- i_q^- + v_d^- i_d^-\right) \\ P_{\cos} = \frac{3}{2}\left(v_q^+ i_q^- + v_d^+ i_d^- + v_q^- i_q^+ + v_d^- i_d^+\right) \\ P_{\sin} = \frac{3}{2}\left(-v_q^+ i_d^- + v_d^+ i_q^- + v_q^- i_d^+ - v_d^- i_q^+\right). \end{cases} \tag{34}$$

The reactive power expression can be written as

$$Q = Q_0 + Q_{\cos}\cos(2\omega_e t + \varphi^+ + \varphi^-) + Q_{\sin}\sin(2\omega_e t + \varphi^+ + \varphi^-) \tag{35}$$

where

$$\begin{cases} Q_0 = \frac{3}{2}\left(v_q^+ i_d^+ - v_d^+ i_d^+ + v_q^- i_d^+ - v_d^- i_d^-\right) \\ Q_{\cos} = \frac{3}{2}\left(v_q^+ i_d^- - v_d^+ i_q^- + v_q^- i_d^+ - v_d^- i_q^+\right) \\ Q_{\sin} = \frac{3}{2}\left(v_q^+ i_q^- + v_d^+ i_d^- - v_q^- i_q^- - v_d^- i_d^+\right). \end{cases} \tag{36}$$

Unlike the balanced case, the steady-state active and reactive powers contain a constant component plus time-varying sine components with a frequency of twice the grid frequency. Also, although six power magnitudes were defined, there only exist four independent currents. Thus, it is only possible to decide the value of four of the six power terms, while the rest depend on the choice of the previous ones. In this situation, it is common to choose to constraint the value of the three components of the active power, which have a direct effect in the evolution of the dc bus voltage, and the mean value of the reactive power. Usually, the reference value for the sine components of the active power is set to be zero to avoid the ripple of the dc bus voltage during unbalanced voltage sags. However, it can also be set to match another time-varying power input as described in [11]. The equations to solve for the power on the grid connection point of the converter are

$$\begin{cases} P_{z0} = \frac{3}{2}(v_{zq}^+ i_{lq}^+ + v_{zq}^- i_{lq}^-) \\ P_{z\cos} = \frac{3}{2}(v_{zq}^+ i_{lq}^- + v_{zq}^- i_{lq}^+) \\ P_{z\sin} = \frac{3}{2}(-v_{zq}^+ i_{ld}^- + v_{zq}^- i_{ld}^+) \\ Q_{z0} = \frac{3}{2}(v_{zq}^+ i_{ld}^+ + v_{zq}^- i_{ld}^-). \end{cases} \tag{37}$$

Solving to obtain the reference current for a given active and reactive power reference, the following relation is obtained

$$\begin{cases} i_{lq}^{+} = \dfrac{2}{3}\left(\dfrac{v_{zq}^{+}}{(v_{zq}^{+})^2-(v_{zq}^{-})^2}P_{z0}^{*} - \dfrac{v_{zq}^{-}}{(v_{zq}^{+})^2-(v_{zq}^{-})^2}P_{z\cos}\right) \\ i_{ld}^{+} = \dfrac{2}{3}\left(\dfrac{v_{zq}^{+}}{(v_{zq}^{+})^2+(v_{zq}^{-})^2}Q_{z0}^{*} + \dfrac{v_{zq}^{-}}{(v_{zq}^{+})^2+(v_{zq}^{-})^2}P_{z\sin}\right) \\ i_{lq}^{-} = \dfrac{2}{3}\left(-\dfrac{v_{zq}^{-}}{(v_{zq}^{+})^2-(v_{zq}^{-})^2}P_{z0}^{*} + \dfrac{v_{zq}^{+}}{(v_{zq}^{+})^2-(v_{zq}^{-})^2}P_{z\cos}\right) \\ i_{ld}^{-} = \dfrac{2}{3}\left(\dfrac{v_{zq}^{-}}{(v_{zq}^{+})^2+(v_{zq}^{-})^2}Q_{z0}^{*} - \dfrac{v_{zq}^{+}}{(v_{zq}^{+})^2+(v_{zq}^{-})^2}P_{z\sin}\right). \end{cases} \tag{38}$$

As in the balanced case, this calculation neglects the difference between the active power in the grid connection point of the converter and the actual active-power output of the inverter. The active power on the inverter terminals can be written as a function of the active power output to the grid as

$$P_{l0} = P_{z0} + r_l((i_{lq}^{+})^2 + (i_{ld}^{+})^2 + (i_{lq}^{-})^2 + (i_{ld}^{-})^2) \tag{39}$$

$$P_{l\cos} = P_{z\cos} + 3r_l(i_{lq}^{+}i_{lq}^{-} + i_{ld}^{+}i_{ld}^{-}) + 3\omega_e L_l(-i_{lq}^{+}i_{ld}^{-} + i_{ld}^{+}i_{lq}^{-}) \tag{40}$$

$$P_{l\sin} = P_{z\sin} - 3r_l(i_{lq}^{+}i_{ld}^{-} - i_{ld}^{+}i_{lq}^{-}) - 3\omega_e L_l(i_{lq}^{+}i_{lq}^{-} + i_{ld}^{+}i_{ld}^{-}). \tag{41}$$

Note that unlike the balanced case, the voltage drop in the inductor not only affects the mean value of the active power, which can be properly compensated by the dc bus voltage controller, but also affects the time-varying terms of the active power, which sometimes are controlled in a open-loop way by setting them to be zero.

As was suggested in the balanced case, one workaround for this problem is to iteratively solve for the current reference by correcting the active-power reference value

$$(i_{lq}^{+})_{n+1} = \frac{2}{3}\frac{v_{zq}^{+}}{(v_{zq}^{+})^2-(v_{zq}^{-})^2}(P_{z0}^{*})_n - \frac{2}{3}\frac{v_{zq}^{-}}{(v_{zq}^{+})^2-(v_{zq}^{-})^2}(P_{z\cos}^{*})_n \tag{42}$$

$$(i_{ld}^{+})_{n+1} = \frac{2}{3}\frac{v_{zq}^{+}}{(v_{zq}^{+})^2+(v_{zq}^{-})^2}Q_{z0}^{*} + \frac{2}{3}\frac{v_{zq}^{-}}{(v_{zq}^{+})^2+(v_{zq}^{-})^2}(P_{z\sin}^{*})_n \tag{43}$$

$$(i_{lq}^{-})_{n+1} = -\frac{2}{3}\frac{v_{zq}^{-}}{(v_{zq}^{+})^2-(v_{zq}^{-})^2}(P_{z0}^{*})_n + \frac{2}{3}\frac{v_{zq}^{+}}{(v_{zq}^{+})^2-(v_{zq}^{-})^2}(P_{z\cos}^{*})_n \tag{44}$$

$$(i_{ld}^{-})_{n+1} = \frac{2}{3}\frac{v_{zq}^{-}}{(v_{zq}^{+})^2+(v_{zq}^{-})^2}Q_{z0}^{*} - \frac{2}{3}\frac{v_{zq}^{+}}{(v_{zq}^{+})^2+(v_{zq}^{-})^2}(P_{z\sin}^{*})_n \tag{45}$$

where

$$(P_{z0}^{*})_n = P_{l0}^{*} - r_l((i_{lq}^{+})_n^2 + (i_{ld}^{+})_n^2 + (i_{lq}^{-})_n^2 + (i_{ld}^{-})_n^2) \tag{46}$$

$$(P_{z\cos}^{*})_n = P_{l\cos}^{*} - 3r_l((i_{lq}^{+})_n(i_{lq}^{-})_n + (i_{ld}^{+})_n(i_{ld}^{-})_n) - 3\omega_e L_l(-(i_{lq}^{+})_n(i_{ld}^{-})_n + (i_{ld}^{+})_n(i_{lq}^{-})_n) \tag{47}$$

$$(P_{z\sin}^{*})_n = P_{l\sin}^{*} + 3r_l((i_{lq}^{+})_n(i_{ld}^{-})_n - (i_{ld}^{+})_n(i_{lq}^{-})_n) + 3\omega_e L_l((i_{lq}^{+})_n(i_{lq}^{-})_n + (i_{ld}^{+})_n(i_{ld}^{-})_n). \tag{48}$$

Finally, one important result from (38), that has not been addressed in previous works is that there exists a discontinuity that causes the reference current to become infinite when $v_{zq}^{+} = v_{zq}^{-}$, i.e., when the magnitude of the positive sequence of the voltage is equal to that of the negative sequence (there is no dominant voltage component). To analyze this particular situation, this condition is introduced in the equation of a unbalanced three-phase signal (22) yielding

$$v_z^{abc}(t) = 2A\begin{bmatrix} \cos\left(\dfrac{\varphi^{+}-\varphi^{-}}{2}\right)\cos\left(\omega_e t + \dfrac{\varphi^{+}+\varphi^{-}}{2}\right) \\ \cos\left(\dfrac{\varphi^{+}-\varphi^{-}}{2} - \dfrac{2\pi}{3}\right)\cos\left(\omega_e t + \dfrac{\varphi^{+}+\varphi^{-}}{2}\right) \\ \cos\left(\dfrac{\varphi^{+}-\varphi^{-}}{2} + \dfrac{2\pi}{3}\right)\cos\left(\omega_e t + \dfrac{\varphi^{+}+\varphi^{-}}{2}\right) \end{bmatrix} \tag{49}$$

where $A \triangleq \sqrt{2}V_z^{+} = \sqrt{2}V_z^{-}$.

From this equation, it can be seen that under such a condition, each phase of v_z^{abc} becomes zero at the same time and it is not possible to get a constant power output from the converter without the need of an infinite current.

One possible solution to this problem would be to limit the result of (38) to a certain value by modulus. One important drawback of this solution is that in this case, it is not possible to assure that the resulting current reference will lead to the desired mean value of the active power, which is critical to maintain the desired mean value of the dc bus voltage.

A different approach based on combining two different reference calculation formulas is possible. The reference calculation expression (38) can be rewritten as

$$\begin{cases} i_{lq}^{+} = \dfrac{2}{3}\dfrac{1}{v_{zq}^{+}}\left(P_{z0}^{*} + \alpha\dfrac{\left(\frac{v_{zq}^{-}}{v_{zq}^{+}}\right)^2 P_{z0}^{*} - \frac{v_{zq}^{-}}{v_{zq}^{+}}P_{z\cos}^{*}}{1-\left(\frac{v_{zq}^{-}}{v_{zq}^{+}}\right)^2}\right) \\ i_{ld}^{+} = \dfrac{2}{3}\dfrac{1}{v_{zq}^{+}}\left(Q_{z0}^{*} + \alpha\dfrac{-\left(\frac{v_{zq}^{-}}{v_{zq}^{+}}\right)^2 Q_{z0}^{*} + \frac{v_{zq}^{-}}{v_{zq}^{+}}P_{z\sin}^{*}}{1+\left(\frac{v_{zq}^{-}}{v_{zq}^{+}}\right)^2}\right) \\ i_{lq}^{-} = \dfrac{2}{3}\dfrac{\alpha}{v_{zq}^{+}}\left(P_{z\cos}^{*} + \dfrac{\left(\frac{v_{zq}^{-}}{v_{zq}^{+}}\right)^2 P_{z\cos}^{*} - \frac{v_{zq}^{-}}{v_{zq}^{+}}P_{z0}^{*}}{1-\left(\frac{v_{zq}^{-}}{v_{zq}^{+}}\right)^2}\right) \\ i_{ld}^{-} = \dfrac{2}{3}\dfrac{\alpha}{v_{zq}^{+}}\left(-P_{z\sin}^{*} + \dfrac{\left(\frac{v_{zq}^{-}}{v_{zq}^{+}}\right)^2 P_{z\sin}^{*} + \frac{v_{zq}^{-}}{v_{zq}^{+}}Q_{z0}^{*}}{1+\left(\frac{v_{zq}^{+}}{v_{zq}^{-}}\right)^2}\right) \end{cases} \tag{50}$$

where α is a parameter that allows switching between two different reference calculation methods. For $\alpha = 1$, (50) becomes equivalent to (38), whereas for $\alpha = 0$, the reference calculation formula becomes

$$\begin{cases} i_{lq}^{+} = \dfrac{2}{3}\dfrac{1}{v_{zq}^{+}} P_{z0}* \\ i_{ld}^{+} = \dfrac{2}{3}\dfrac{1}{v_{zq}^{+}} Q_{z0}* \\ i_{lq}^{-} = 0 \\ i_{ld}^{-} = 0. \end{cases} \tag{51}$$

This equation is equivalent to the one used for the conventional vector control meant for the balanced operation; thus, the references for the negative-sequence current are zero. From (37), it can be seen that this produces the desired mean value for the active and the reactive power but does not allow for the control of the sine time-varying terms of the active power.

One important remark that can be made by comparing (51) and (38) is that, in general, in the case of the existence of negative-sequence voltages in the grid, the suppression of the active-power oscillation by injecting negative current leads to a reduction of the mean value of the active power. This in turn leads to the need of a higher positive-sequence current to maintain the mean value of the active power. Thus, in case of a voltage sag, where usually the maximum allowed current becomes an issue, (38) is more likely to have a problem extracting the needed active power to maintain the desired dc bus voltage. On the other hand, as the effect of the power oscillation on the dc bus voltage is directly related to the capacitance of the dc-side capacitor filter, this suggests that systems that use a dc-side capacitor filter with a small value of capacitance, which may be the standard practice in HVdc link systems, it may be necessary to overrate the current capability of the inverter to be able to compensate for the oscillations in the case of a network unbalance.

V. Simulation Testing of the Proposed Reference Calculation Scheme

In order to test the performance of the proposed control methods, a simulation of the response of the system to an unbalanced voltage sag is performed. The characteristic parameters of the simulated converter and the operation point for the simulation can be found in Table I. The rating of the converter and its switching frequency is the same as the grid-side inverter of the rotor converter of the 1-MW DFIG wind turbine in [19]. The machine-side inverter has been modeled as a constant power input of 300 kW with no ripple. Thus, the power references for $P_{l\sin}$ and $P_{l\cos}$ will be set to zero to avoid the ripple of the dc bus voltage.

The response of the system to an unbalanced voltage sag is simulated using three different calculation methods (see Fig. 2). The first one, referred to as Method I, uses the formula presented in (50) for $\alpha = 0$, the second one, referred to as Method II, uses the presented formula in (50) for $\alpha = 1$ plus the iterative compensation of the filter impedance, and the third one, referred to as Method III, uses the same formula as that of Method II but without compensating the filter impedance.

TABLE I
Characteristic Parameters of the Simulated Scenario

Parameter	Units	Value	Description
V_z^N	690	V	Grid nominal voltage
P_l^N	300	kW	Nominal active power
Q_z^N	100	kVAr	Nominal reactive power
V_{DC}^N	1338	V	DC bus nominal voltage
r_l	0.05	Ω	Grid connection filter resistance
L_l	27	mH	Grid connection filter inductance
f_s	3	kHz	Inverter switching frequency
T_i	50	ms	Current control settling time
T_{PLL}	20	ms	Grid voltage PLL settling time

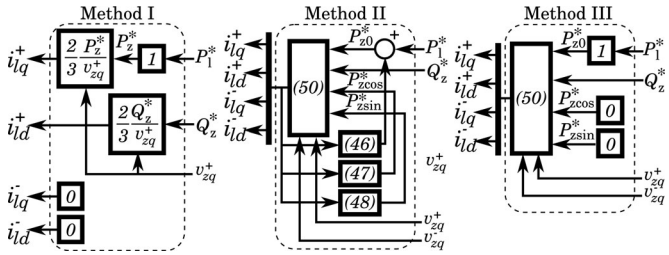

Fig. 2. Current reference calculation methods.

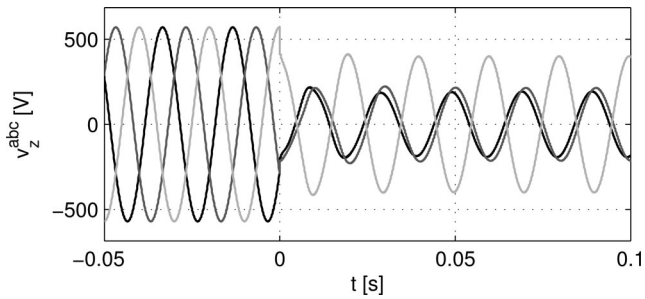

Fig. 3. Voltage at the PCC of the converter.

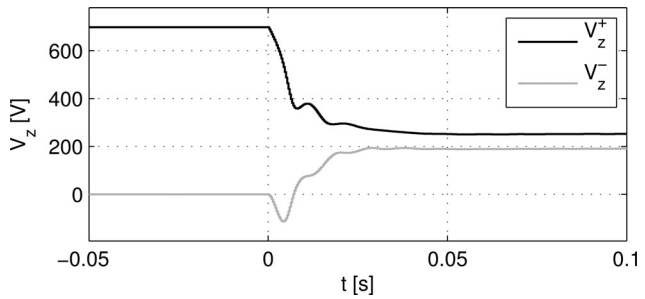

Fig. 4. Amplitude of the positive and negative sequences of the voltage at the PCC measured by the PLL.

The simulated voltage sag corresponds to a two phase to ground sag, which causes the voltage of two of the phases to drop by 65%. The waveform of the grid voltage seen by the inverter is shown in Fig. 3 and the amplitude of the positive and negative sequences as measured by the PLL used by the controller is shown in Fig. 4. Note that this sag causes the positive sequence

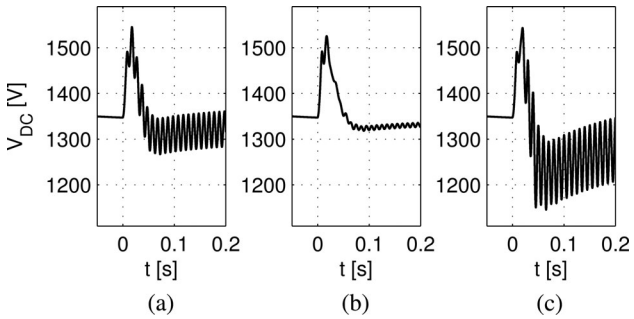

Fig. 5. Comparison of the evolution of the dc bus voltage using current reference calculation methods (a) Method I, (b) Method II, and (c) Method III.

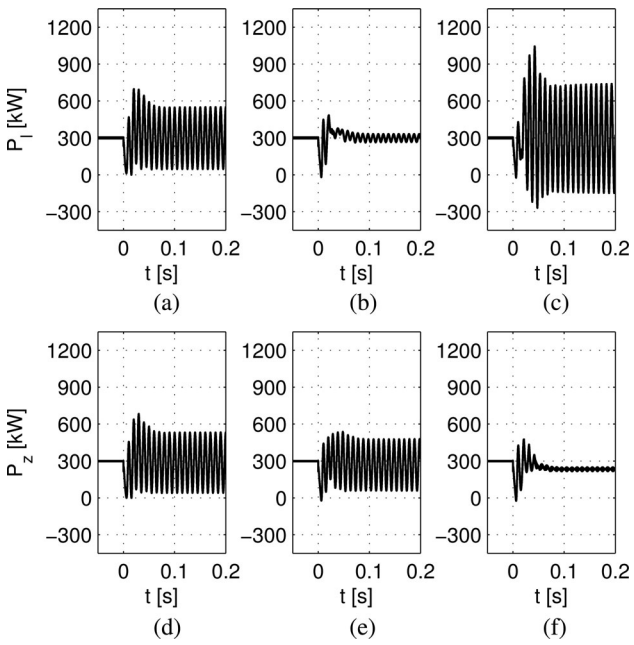

Fig. 6. Comparison of the evolution of the converter output power measured on the inverter versus the power measured on the PCC using current reference calculation methods (a), (d) Method I; (b), (e) Method II; and (c), (f) Method III.

of the voltage to reduce to 0.36 pu and the negative sequence to appear with an amplitude of 0.30 pu; thus, the ratio between the positive- and the negative-sequence amplitudes is 1.2, which is close to 1.0, the limit of Methods II and III.

The controller used in the simulation model uses the double synchronous reference frame (DSRF) current controller described in [11] and a PLL for unbalanced voltages described in [20]. The performance specifications for both parts of the controller can be found in Table I.

Fig. 5 shows the evolution of the voltage during the sag. Notice that the initial transient is the same for all the methods as expected but the steady state differs. Methods I and III produce a significant steady-state ripple; the reason for that is that Method I does not use negative sequence and Method III does not compensate the difference between the power on the grid connection point and the power on the inverter terminals. This can further be confirmed by plotting P_l and P_z (see Fig. 6). Notice that Method III allows to suppress the ripple in P_z but causes an

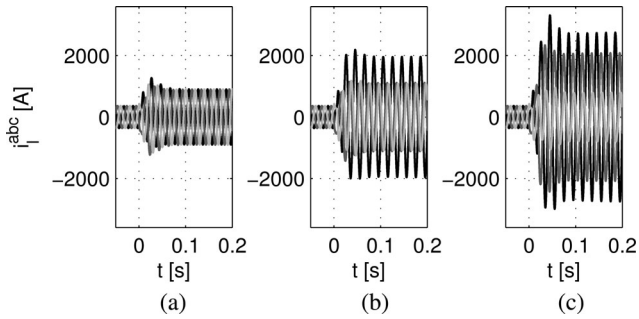

Fig. 7. Comparison of the output current of the converter using current reference calculation methods (a) Method I, (b) Method II, and (c) Method III.

important ripple in P_l, which makes the dc bus voltage to have a larger oscillation than Method I.

The evolution of the current is shown in Fig. 7. Note that all methods require an increase of the current due to the reduction of the voltage. Also, as noted before, Methods II and III require more current than Method I even though the oscillation in Method III is larger than in Method I.

VI. Experimental Testing of the Proposed Reference Calculation Scheme

In order to further verify the theoretical results, a test of the analyzed current reference calculation schemes is performed on an experimental platform. The test platform consists of two CDM2480 [21] low power voltage source three-phase inverters fed by two independent 24-V dc buses and connected by the ac side through a three-phase inductor ($r = 0.1\ \Omega$, $L = 4.9$ mH). One of the inverters, referred to as the generator grid-side inverter, is used to emulate the grid-side inverter of a grid-connected power source and inject power from its dc bus to the other inverter, referred to as the grid emulator, used to emulate the behavior of the grid. A picture and a diagram of the different parts of the experimental setup can be seen in Fig. 8. The voltage of the terminals of the generator side inverter and the grid emulator and the current flowing through the inductors are measured and recorded using a data adquisition device.

Each inverter is controlled by a TMS320F2812 eZdsp control board, which have been programmed for the test. The grid emulator inverter is programmed to apply three-phase voltage waveforms on its ac side corresponding to those of the two phase fault used in the simulations in the previous section regardless of the current flowing through it, thus emulating the behavior of a strong grid. The grid-side converter is controlled using a DSRF closed-loop current controller able to follow unbalanced current reference values as in the simulated scenario of the previous section.

Three different tests starting from the same operation point are performed on the experimental platform using a different current reference calculation method each time. The response of the system to an unbalanced voltage sag is observed for a given reference value of the average active power injected to the grid using the three reference calculation methods referred as Method I (injecting only positive sequence current), Method II (injecting unbalanced current to suppress the active power ripple

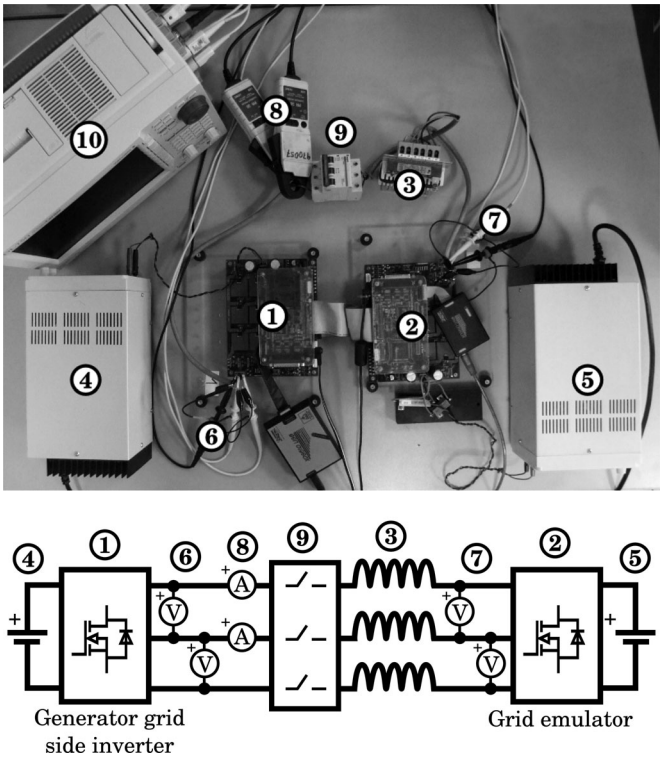

Fig. 8. Picture and schematics of the experimental setup: (1) generator grid-side inverter, (2) grid emulator, (3) converter inductances, (4) generator-side dc power source, (5) grid emulator dc power source and load, (6) generator grid-side inverter voltage v_l^{abc} measurement, (7) grid emulator voltage v_z^{abc} measurement, (8) generator grid-side output current i_l^{abc} measurement, (9) grid connection switch, (10) data adquisition device.

plus the effect of the filter impedance), and Method III (injecting unbalanced current to suppress the active power ripple in the point of connection of the converter to the grid). The voltage sag is chosen to resemble that of the simulated scenario of the previous section, where the amplitude of the positive sequence of the voltage is close to the value of the negative sequence of the voltage.

The evolution of the grid voltage, the current and the active power flowing through the converter and the active power injected to the grid for each scheme can be seen in Figs. 9–11. It can be seen, as expected, that all three methods obtain the desired average active-power injection during the sag requiring an increase of the current to keep the same average power output from the converter in any case. In the case of Method I, the current during the voltage sag is higher but symmetrical for each phase, whereas Methods II and III require asymmetrical currents that are not only higher than the current needed in normal operation but they are also higher than the current needed using Method I in at least one of the phases.

Regarding the power ripple, Method I produces an important ripple that is equal in the converter terminal as in the point of connection to the grid. The reason for this can be seen in (34), as the negative-sequence current is zero, the power ripple only depends on the interaction between the positive-sequence current and the negative-sequence voltage, as the negative-sequence voltage is the same in the grid as in the converter (as there is no

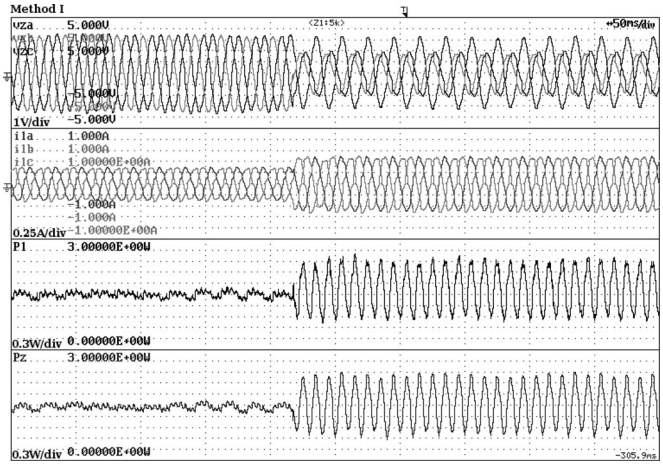

Fig. 9. Experimental results for Method I. From top to bottom: v_z^{abc}, i_l^{abc}, P_l, and P_z.

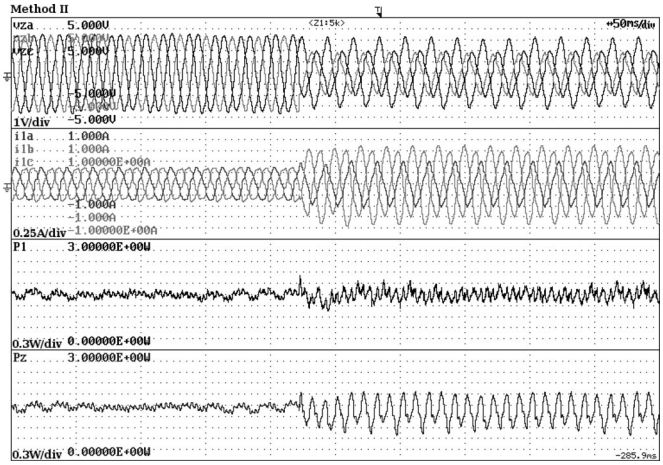

Fig. 10. Experimental results for Method II. From top to bottom: v_z^{abc}, i_l^{abc}, P_l, and P_z.

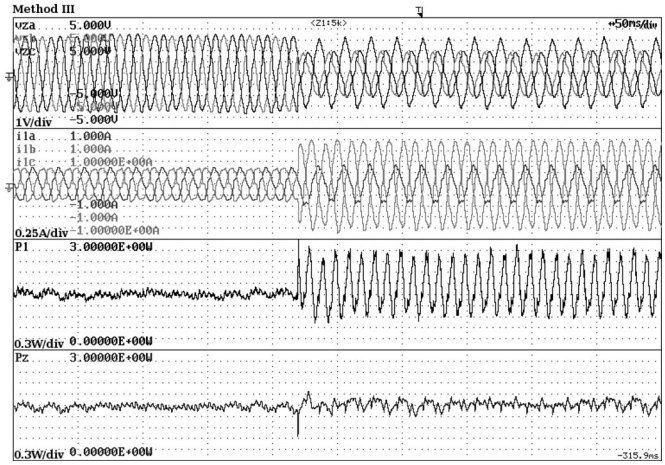

Fig. 11. Experimental results for Method III. From top to bottom: v_z^{abc}, i_l^{abc}, P_l, and P_z.

negative-sequence current flowing through the impedance), the ripple is equal in both points.

Method III is able to compensate the ripple in the power injected to the grid but it produces an important ripple in the converter output power. By using the proposed iterative calculation to calculate the current reference to compensate for the effect of the inductor impedance, Method II is able to suppress that ripple but then a ripple appears in the power injected to the grid.

Thus, comparing the three methods, the one that requires a lower current is Method I even though as a drawback it produces a ripple in the current flowing through the converter during unbalanced faults. On the other hand, Method II has been shown to be the only method capable of suppressing the oscillations of the active power although it requires a larger current for the same average active power. Finally, Method III is unable to suppress the oscillation due to the neglection of the effect of the filter impedance of the converter. Thus, the iterative reference calculation used in Method II is needed in order to properly compensate the power ripple during unbalanced voltage sags.

VII. Conclusion

The injection of negative-sequence currents has been shown to suppress the oscillation on the dc bus voltage due to the oscillation of the power injected to the grid during a unbalanced voltage sag. However, compared to the standard method of injecting only the positive-sequence current, this method has been found to require larger currents to maintain the same level of average active power. For deep voltage sags, this may lead to even higher oscillations of the dc bus voltage if the effect of the ac filter impedance on the converter power output is not properly compensated and a method has been proposed to do it. Also, a special condition has been identified which makes it impossible to control the oscillating terms of the active power and a solution for the calculation of the current references in that case has been proposed.

References

[1] C. Sao and P. Lehn, "Control and power management of converter fed microgrids," *IEEE Trans. Power Syst.*, vol. 23, no. 3. pp. 1088–1098, Aug. 2008.

[2] O. Gomis-Bellmunt, J. Liang, J. Ekanayake, R. King, and N. Jenkins, "Topologies of multiterminal HVDC–VSC transmission for large offshore wind farms," *Electr. Power Syst. Res.*, vol. 81, pp. 271–281, 2011.

[3] V. Blasko and V. Kaura, "A new mathematical model and control of a three-phase ac–dc voltage source converter," *IEEE Trans. Power Electron.*, vol. 12, no. 1, pp. 116–123, Jan. 1997.

[4] S. Buso, *Digital Control in Power Electronics (Synthesis Lectures on Power Electronics)*. Seattle, WA: Morgan and Claypool Publishers, 2006.

[5] M. H. Bollen, *Understanding Power Quality Problems: Voltage Sags and Interruptions*. Piscataway, NJ: Wiley-IEEE Press, 1999.

[6] J. Morren and S. de Haan, "Ridethrough of wind turbines with doubly fed induction generator during a voltage dip," *IEEE Trans. Energy Convers.*, vol. 20, no. 2, pp. 435–441, Jun. 2005.

[7] C. Feltes, H. Wrede, F. Koch, and I. Erlich, "Enhanced fault ride-through method for wind farms connected to the grid through VSC-based HVDC transmission," *IEEE Trans. Power Syst.*, vol. 24, no. 3, pp. 1537–1546, Aug. 2009.

[8] L. Xu, "Coordinated control of DFIG's rotor and grid side converters during network unbalance," *IEEE Trans. Power Electron.*, vol. 23, no. 3, pp. 1041–1049, May 2008.

[9] H. Song and K. Nam, "Dual current control scheme for PWM converter under unbalanced input voltage conditions," *IEEE Trans. Ind. Electron.*, vol. 46, no. 5, pp. 953–959, Oct. 1999.

[10] P. Rioual, H. Pouliquen, and J.-P. Louis, "Regulation of a PWM rectifier in the unbalanced network state using a generalized model," *IEEE Trans. Power Electron.*, vol. 11, no. 3, pp. 495–502, May 1996.

[11] O. Gomis-Bellmunt, A. Junyent-Ferre, A. Sumper, and J. Bergas-Jané, "Ride-through control of a doubly fed induction generator under unbalanced voltage sags," *IEEE Trans. Energy Convers.*, vol. 23, no. 4, pp. 1036–1045, Dec. 2008.

[12] S. Alepuz, S. Busquets-Monge, J. Bordonau, J. Martinez-Velasco, C. C. A. Silva, J. Pontt, and J. Rodriguez, "Control strategies based on symmetrical components for grid-connected converters under voltage dips," *IEEE Trans. Ind. Electron.*, vol. 56, no. 6, pp. 2162–2173, Jun. 2009.

[13] Y. Zhou, P. Bauer, J. Ferreira, and J. Pierik, "Operation of grid connected dfig under unbalanced grid voltage condition," *IEEE Trans. Energy Convers.*, vol. 24, no. 1, pp. 240–246, Mar. 2009.

[14] J. Hu, Y. He, L. Xu, and B. Williams, "Improved control of dfig systems during network unbalance using PIR current regulators," *IEEE Trans. Ind. Electron.*, vol. 56, no. 2, pp. 439–451, Feb. 2009.

[15] Z. Li, Y. Li, P. Wang, H. Zhu, C. Liu, and W. Xu, "Control of three-phase boost-type PWM rectifier in stationary frame under unbalanced input voltage," *IEEE Trans. Power Electron.*, vol. 25, no. 10, pp. 2521–2530, Oct. 2010.

[16] C.-M. Ong, *Dynamic Simulations of Electric Machinery: Using MATLAB/SIMULINK*. Englewood Cliffs, NJ: Prentice-Hall, 1997.

[17] C. L. Fortescue, "Method of symmetrical co-ordinates applied to the solution of polyphase networks," *Amer. Inst. Electr. Eng., Trans.*, vol. XXXVII, no. 2, pp. 1027–1140, 1918.

[18] H. Akagi, E. H. Watanabe, and M. Aredes, *Instantaneous Power Theory and Applications to Power Conditioning (IEEE Press Series on Power Engineering)*. Hoboken, NJ: Wiley-IEEE Press, 2007.

[19] A. Junyent-Ferré, O. Gomis-Bellmunt, A. Sumper, M. Sala, and M. Mata, "Modeling and control of the doubly fed induction generator wind turbine," *Simul. Model. Practice Theory*, vol. 18, no. 9, pp. 1365–1381, 2010.

[20] M. Karimi-Ghartemani and H. Karimi, "Processing of symmetrical components in time-domain," *IEEE Trans. Power Syst.*, vol. 22, no. 2, pp. 572–579, May 2007.

[21] D. Montesinos, S. Galceran, A. Sudria, and O. Gomis, "A laboratory test bed for PM brushless motor control," in *Proc. Eur. Conf. Power Electron. Appl.*, Dresden, Germany, 2005.

Adrià Junyent-Ferré (S'09) received the B.Sc. and M.Sc. Ind. Eng. degrees from the School of Industrial Engineering of Barcelona (ETSEIB), Technical University of Catalonia (UPC), Barcelona, Spain, in 2007, and the Ph.D. degree in electrical engineering from the UPC in 2011.

He has been with the Centre of Technological Innovation in Static Converters and Drives of the UPC since 2006. His current research interests include the control of power electronic converters, renewable generation systems, and electrical machines.

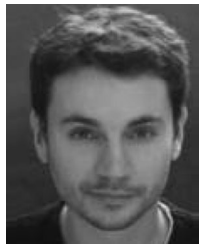

Oriol Gomis-Bellmunt (S'05–M'07) received the B.Sc. and M.Sc. Ind. Eng. degrees from the School of Industrial Engineering of Barcelona (ETSEIB), Technical University of Catalonia (UPC), Barcelona, Spain, in 2001 and the Ph.D. degree in electrical engineering from the UPC in 2007.

In 1999, he joined Engitrol S.L., where he worked as the Project Engineer in the automation and control industry. In 2003, he developed part of his Ph.D. thesis in the DLR (German Aerospace center), Braunschweig, Germany. Since 2004, he has been a Lecturer with the Department of Electrical Engineering, UPC where he participates in the Centre of Technological Innovation in Static Converters and Drives of the UPC research group. Also, since 2009, he has been with the Catalonia Institute for Energy Research (IREC), Barcelona, Spain. His research interests include the fields linked with smart actuators, electrical machines, power electronics, renewable energy integration in power systems, industrial automation, and engineering education.

Tim C. Green (SM'03) received the B.Sc. Eng. degree (first class Hons.) from Imperial College, London, U.K., in 1986, and the Ph.D. degree from Heriot-Watt University, Edinburgh, U.K., in 1990, both in electrical engineering.

He was a Lecturer at Heriot-Watt University until 1994. He is now a Professor of electrical power engineering at Imperial College London and the Deputy Head of the Department of Electrical and Electronic Engineering. He leads the HubNet consortium of eight U.K. universities researching future energy networks. His research interests include formulation of electricity networks that support low-carbon futures, the use of power electronics and control to accommodate new generation patterns and new forms of load, such as EV charging as part of the emerging smart grid. He has particular interests in offshore dc networks and of management of low voltage networks.

Dr. Green is a Chartered Engineer in the U.K.

Diego E. Soto-Sanchez (M'95) received the B.Sc. Electr. Eng. degree from the University of Magallanes, Chile, in 1990, and the Ph.D. degree from Imperial College, London, U.K., in 1999.

Since 1990, he has been a Lecturer in power electronics and drives in the Department of Electrical Engineering, University of Magallanes, Chile. He is currently a Research Associate at Imperial College London, involved in the research on multiterminal high voltage direct current (HVdc) systems. His research interests include high power converters for FACTS and HVdc systems.